Supplemental Figures

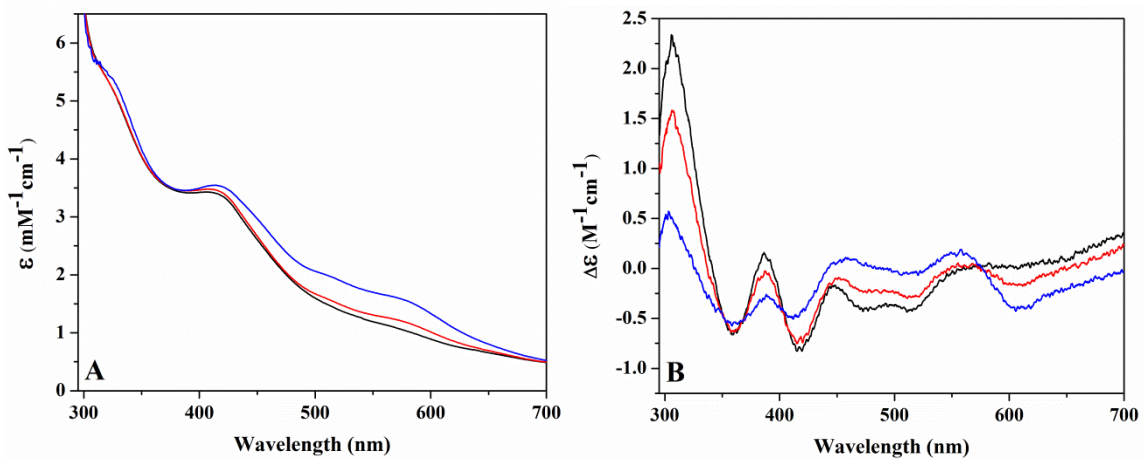

Figure S1. Changes in spectroscopic properties accompanying successive freeze/thaw events for a single sample of HydF. **A**. UV-visible absorbance changes for freshly purified HydF (152 μM protein at 2.34 ± 0.10 Fe/dimer; black), freshly purified enzyme following a single freeze-thaw event (red), and freshly purified enzyme following a second freeze-thaw event (blue). ε values are reported for total Fe concentration in sample. **B**. The corresponding circular dichroism spectra for the UV-vis spectra represented in panel **A** (color scheme is consistent); Δε values shown are for total iron content in samples.

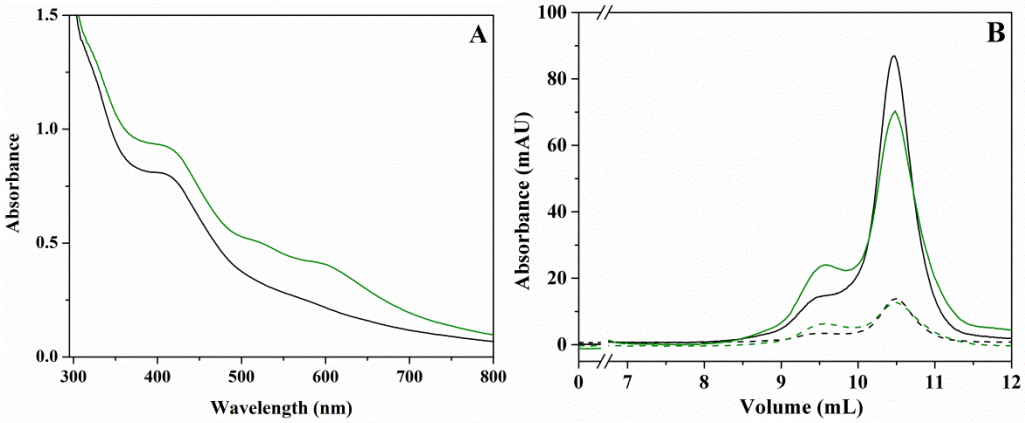

Figure S2. Changes in visible absorbance and oligomeric state upon sample handling of freshly purified HydF. **A**. UV-visible absorbance spectra for freshly purified HydF (black, peak fraction, 99 μM protein at 2.18 ± 0.08 Fe/dimer) and freshly purified HydF after concentration (green, side fractions pooled and concentrated, 102 μM protein at 2.48 ± 0.06 Fe/dimer). Side fractions were pooled together and concentrated using a Minicon B15 sponge well concentrator prior to UV-Vis and gel filtration analysis without undergoing a freeze/thaw event. **B**. The corresponding gel filtration data for the samples in **A** (color scheme is consistent between panels); for Panel B, the solid trace represents the signal at 280 nm, and the dashed trace represents the signal at 426 nm.

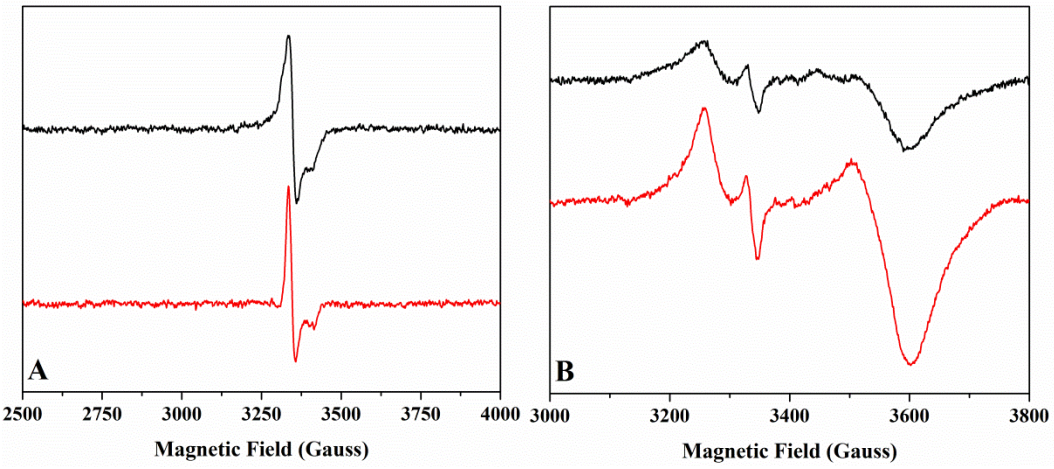

Figure S3. Representative CW X-band EPR spectra for freshly purified HydF. **A**. EPR spectra for freshly purified HydF (red, 111 μM protein at 2.50 ± 0.08 Fe/dimer) relative to freshly purified HydF that has been concentrated (black, 102 μM protein at 2.48 ± 0.06 Fe/dimer; see data and sample description provided in Figure S2). **B**. Photoreduced EPR spectra of the samples represented in panel **A** (red, 110 μM protein at 2.50 ± 0.08 Fe/dimer; black, 97 μM protein at 2.48 ± 0.06 Fe/dimer). All spectra recorded at 12 K with 1 mW microwave power.

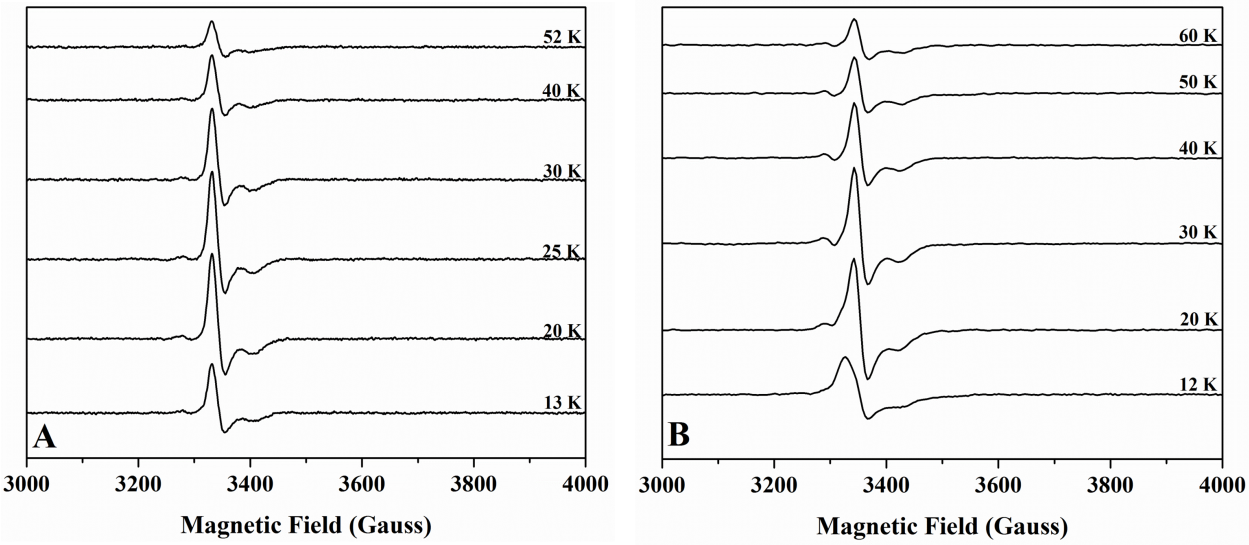

Figure S4. CW EPR (X-band) temperature relaxation profiles for HydF. **A**. Temperature relaxation profile for freshly purified HydF (111 μM protein at 2.50 ± 0.08 Fe/dimer) at 1 mW microwave power setting. The magnitude of the signal intensity (S.I., defined as the absolute value of the g ~ 2.00 peak-to-peak feature) at each temperature value is provided. **B**. Temperature relaxation profile for as-isolated HydF (600 μM protein at 1.14 ± 0.08 Fe/dimer) at 1 mW microwave power setting.

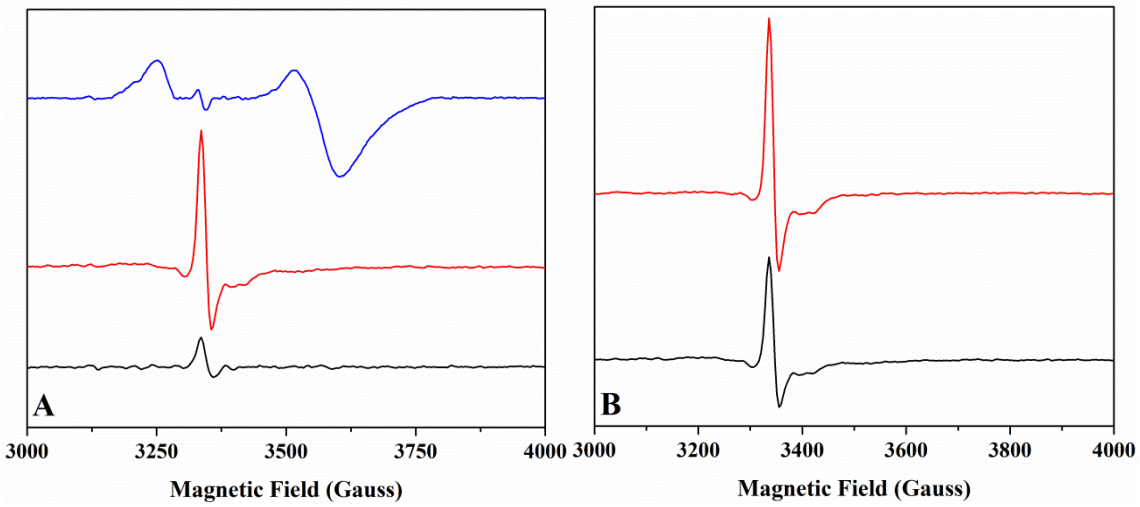

Figure S5. EPR spectra showing the effects of exogenous reducing agents on freshly purified HydF. **A**. The enzyme freshly purified in the absence of reducing agents (black), in the presence of 5 mM dithiothreitol (red), and in the presence of 5 mM dithionite (blue). All samples used 104 μM protein at 2.18 ± 0.08 Fe/dimer. Freshly purified and DTT spectra were recorded at 16 K, while the DT treated sample was recorded at 10.5 K. **B**. The signal of the DTT treated sample at 16 K (black) and 30 K (red) at 1 mW microwave power.

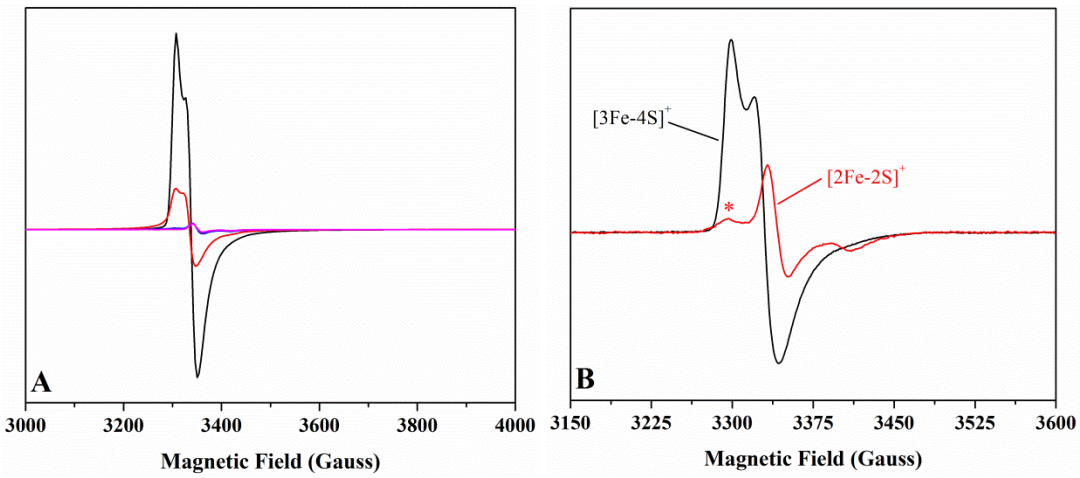

Figure S6. Low temperature CW (X-band) EPR spectroscopy of as-purified PFL-AE (1.68 mM protein with 2.70 ± 0.10 Fe/protein). **A**. Temperature relaxation profile (black, 12K; red, 20 K; blue, 30 K; magenta, 40 K). **B**. Overlay of the $[3Fe\text{-}4S]^+$ (black) and $[2Fe\text{-}2S]^+$ (red) cluster signals in PFL-AE at low power settings. The $[3Fe\text{-}4S]^+$ cluster signal was recorded at 12 K and 63 μW microwave power using a gain setting of $1x10^2$. The $[2Fe\text{-}2S]^+$ cluster signal was recorded at 30 K and 63 μW microwave power using a gain setting of 1×10^3. The red asterisk denotes residual $[3Fe\text{-}4S]^+$ content in the 30 K spectrum.

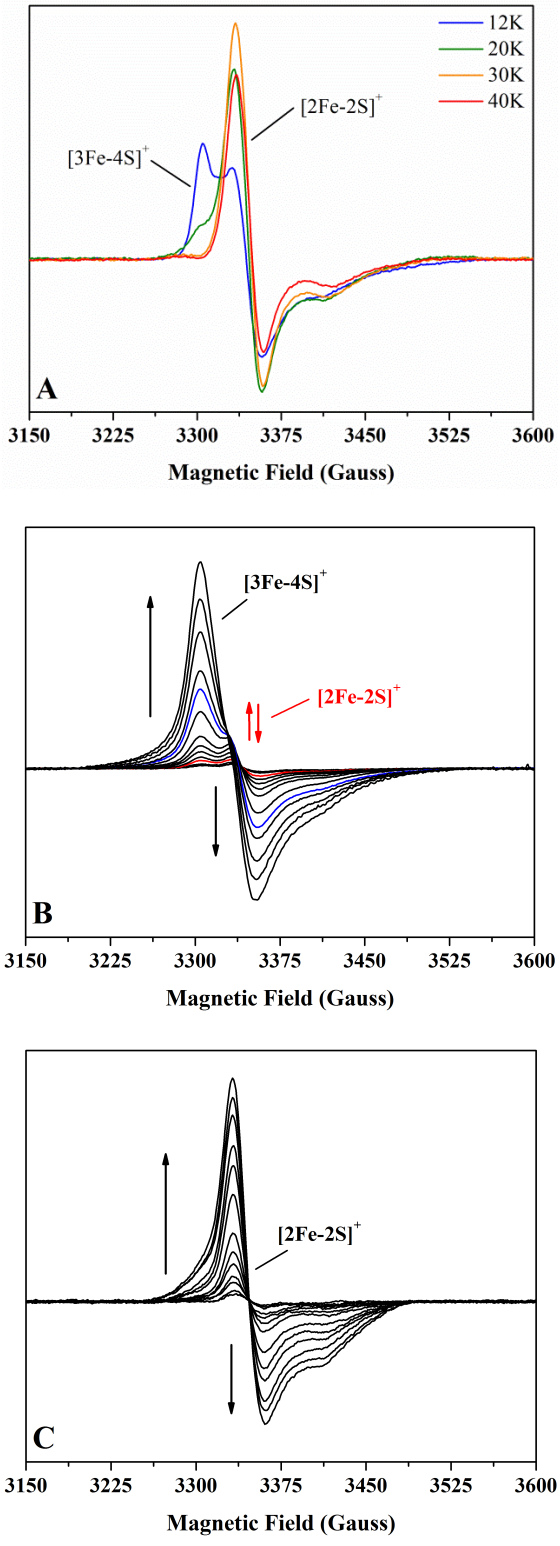

Figure S7. Low temperature CW X-band EPR spectra of as-reconstituted HydE. **A**. Temperature relaxation behavior of as-reconstituted enzyme. The $[3Fe\text{-}4S]^+$ component of the signal at 12 K rapidly relaxes as temperature is raised concomitant with the intensification of the $[2Fe\text{-}2S]^+$ component. **B**. The effects of increasing microwave power (12 μW – 50 mW) on the

$[3Fe\text{-}4S]^{+}$ and $[2Fe\text{-}2S]^{+}$ cluster signals of as-reconstituted HydE at 12 K. The red highlighted spectrum shows the $[2Fe\text{-}2S]^{+}$ component signal at 63 μW whose signal intensity increases and then decreases as a function of power (red arrows); the blue highlighted spectrum is at 6 mW power where the $[2Fe\text{-}2S]^{+}$ component signal exhibits substantial saturation effects. The signal intensity of the $[3Fe\text{-}4S]^{+}$ cluster, which steadily grows as a function of increasing power, is highlighted by the black arrows. **C**. The effects of increasing microwave power (12 μW – 50 mW) on the $[2Fe\text{-}2S]^{+}$ cluster signal of as-reconstituted HydE at 30 K. The signal intensity of the $[2Fe\text{-}2S]^{+}$ cluster, which steadily increases as a function of increasing power, is highlighted by the black arrows. For all panels, HydE enzyme was 344 μM protein at 7.64 ± 0.10 Fe/protein.

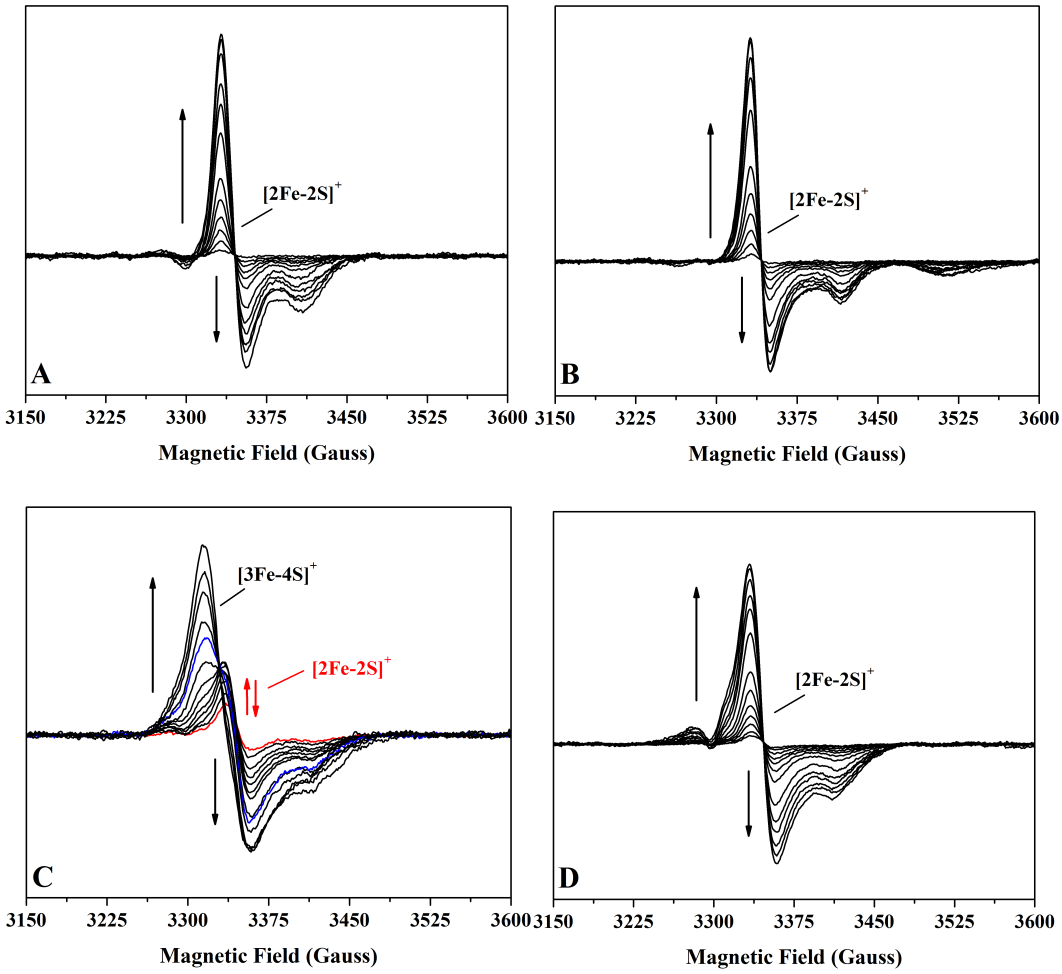

Figure S8. Low temperature, CW X-band EPR spectra of HydF as a function of varying microwave power settings. **A**. The $[2Fe\text{-}2S]^+$ cluster signal in freshly purified HydF as a function of increasing microwave power (31 μW – 50 mW) recorded at 30 K (111 μM protein at 2.50 ± 0.08 Fe/dimer). The signal intensity of the $[2Fe\text{-}2S]^+$ cluster, which steadily increases as a function of increasing power, is highlighted by the black arrows. **B**. The $[2Fe\text{-}2S]^+$ cluster signal in freshly purified, photoreduced HydF as a function of increasing microwave power (31 μW – 50 mW) recorded at 30 K (110 μM protein at 2.50 ± 0.08 Fe/dimer). The feature present at ~ 3525 G is residual $[4Fe\text{-}4S]^+$ cluster signal. The signal intensity of the $[2Fe\text{-}2S]^+$ cluster, which steadily increases as a function of increasing power, is highlighted by the black arrows. **C**. The effects of increasing microwave power (12 μW – 50 mW) on the $[3Fe\text{-}4S]^+$ and $[2Fe\text{-}2S]^+$ cluster signals of as-isolated HydF at 15 K (600 μM protein at 1.14 ± 0.08 Fe/dimer). The red highlighted spectrum shows the $[2Fe\text{-}2S]^+$ component signal at 12 μW whose signal intensity increases and then decreases as a function of power (red arrows); the blue highlighted spectrum is at 6 mW power where the $[2Fe\text{-}2S]^+$ component signal exhibits substantial saturation effects. The signal intensity of the $[3Fe\text{-}4S]^+$ cluster, which steadily grows as a function of increasing power, is highlighted by the black arrows. **D**. The effects of increasing microwave power (12 μW – 50 mW) on the $[2Fe\text{-}2S]^+$ cluster signal of as-isolated HydF at 30 K (600 μM protein at

1.14 ± 0.08 Fe/dimer). The signal intensity of the $[2Fe\text{-}2S]^{+}$ cluster, which steadily grows as a function of increasing power, is highlighted by the black arrows.

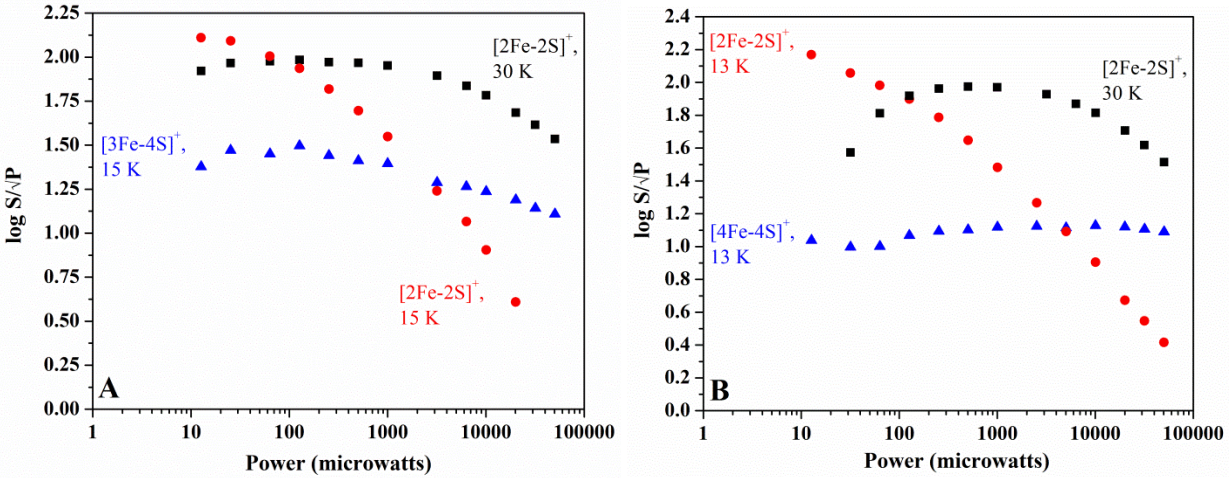

Figure S9. EPR microwave power saturation curves for HydF qualitatively comparing $[2Fe\text{-}2S]^{+}$, $[3Fe\text{-}4S]^{+}$, and $[4Fe\text{-}4S]^{+}$ cluster signal behavior. **A**. As-isolated HydF (600 μM protein at 1.14 ± 0.08 Fe/dimer) FeS cluster states. **B**. Photoreduced, freshly purified HydF (110 μM protein at 2.50 ± 0.08 Fe/dimer) FeS cluster states.

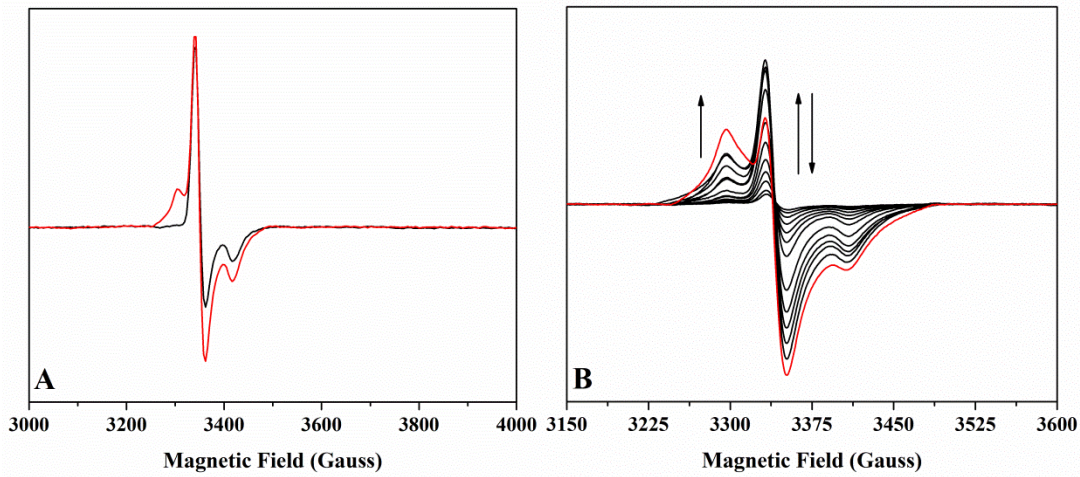

Figure S10. Low temperature CW X-band EPR spectroscopy of as-purified PFL-AE (1.68 mM protein with 2.70 ± 0.10 Fe/protein). **A**. Temperature relaxation behavior recorded at 1 mW microwave power and either 30 K (red) or 40 K (black) highlighting the disappearance of the $[3Fe\text{-}4S]^{+}$ g = 2.035 feature. **B**. Spectral changes at 30 K for the $[3Fe\text{-}4S]^{+}$ and $[2Fe\text{-}2S]^{+}$ cluster signals in PFL-AE as a function of increasing microwave power (12 μW – 50 mW). The red spectrum highlights the 50 mW data wherein the $[3Fe\text{-}4S]^{+}$ cluster signal at g = 2.035 continues to increase in signal intensity, whereas the g ~ 2.0 centered $[2Fe\text{-}2S]^{+}$ cluster begins to visibly show saturation behavior. Collectively this data provided support for the assignment of two paramagnetic species present in the 30 K data which in turn aided spectral simulations (see Figure S11).

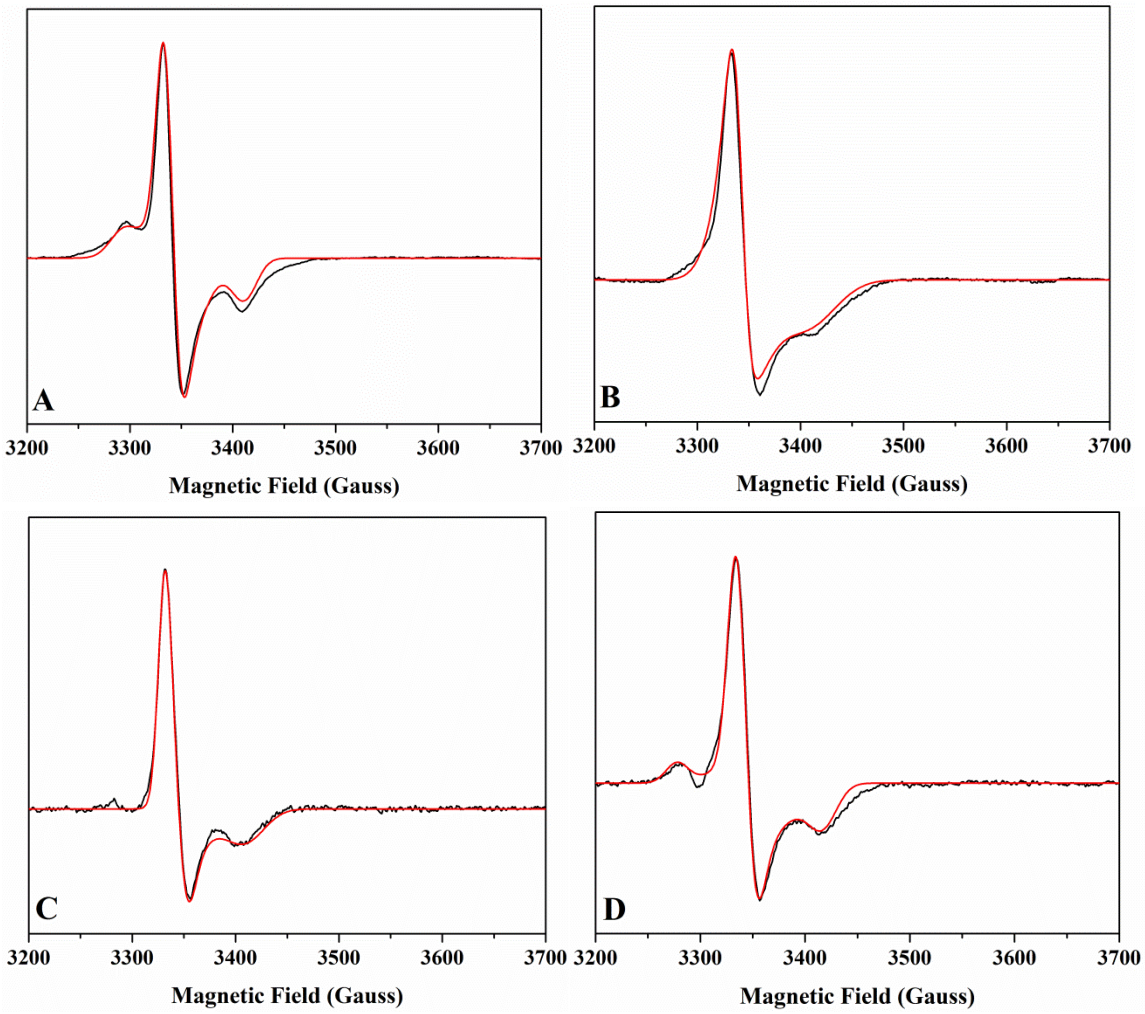

Figure S11. EasySpin spectral simulations of $[2Fe\text{-}2S]^{+}$ cluster signals as observed at 30 K and 1 mW microwave power. In all panels, experimental data are shown in black while spectral simulations are represented in red. **A**. As-isolated PFL-AE (1.68 mM protein with 2.70 ± 0.10 Fe/protein). The experimental spectrum is simulated as components of $[2Fe\text{-}2S]^{+}$ and $[3Fe\text{-}4S]^{+}$ cluster signals (see Figure S6 and Figure S10). **B**. As-reconstituted HydE (344 μM protein at 7.64 ± 0.10 Fe/protein). The experimental spectrum is simulated as a single $[2Fe\text{-}2S]^{+}$ cluster signal. **C**. Freshly purified HydF (111 μM protein at 2.50 ± 0.08 Fe/dimer). The experimental spectrum is simulated as a single $[2Fe\text{-}2S]^{+}$ cluster signal. **D**. As-isolated HydF (600 μM protein at 1.14 ± 0.08 Fe/dimer). The experimental spectrum is simulated as two distinct $[2Fe\text{-}2S]^{+}$ cluster signals (see discussion in main text).

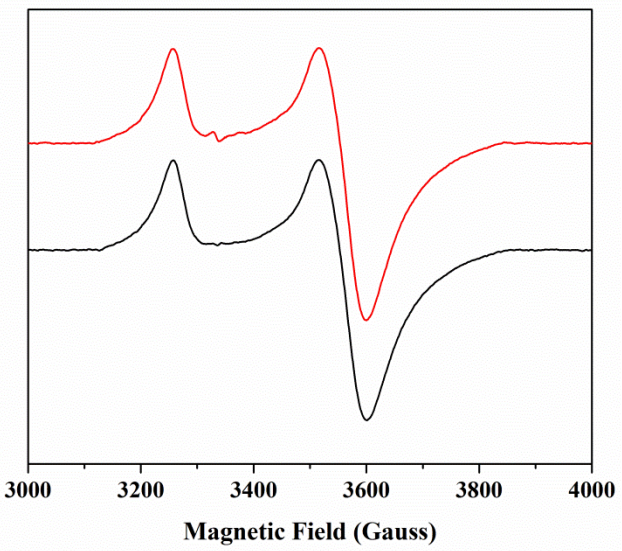

Figure S12. Low temperature CW X-band EPR monitoring the effects of 5 mM dithionite on HydF's FeS cluster signals. As-isolated, dithionite reduced HydF (72 μM protein at 2.54 ± 0.04 Fe/dimer) before (black) and after (red) a thaw/freeze event. Spectra recorded at 10.5 K.

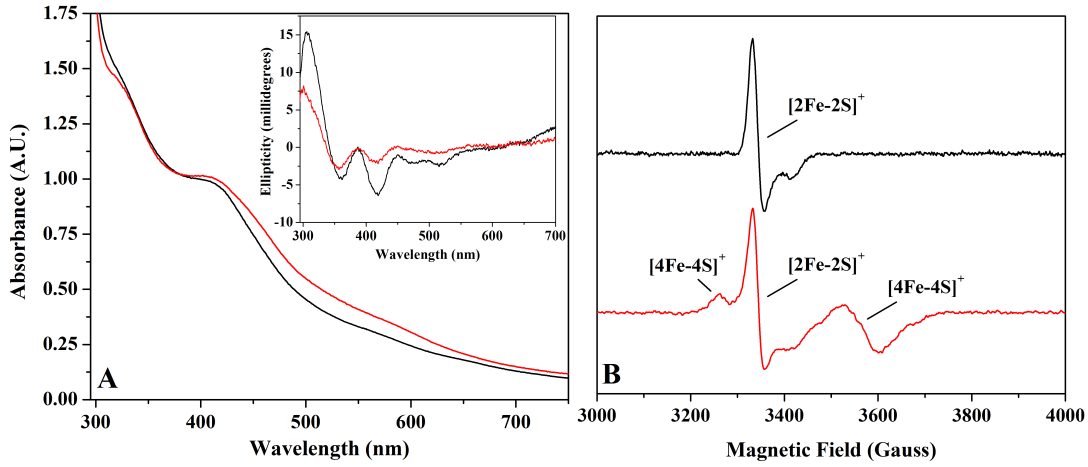

Figure S13. Changes in spectroscopic properties accompanying a freeze/thaw event in freshly purified HydF following gel filtration. **A**. UV-visible absorbance changes for HydF before (black; 71 μM protein at 3.10 ± 0.11 Fe/dimer) and after a single freeze-thaw event (red). *Inset*. The corresponding circular dichroism spectra for the UV-vis data (the color scheme for spectra is consistent). **B**. Low temperature, CW X-band EPR spectra for freshly purified HydF following gel filtration. Freshly purified enzyme (68 μM protein at 3.10 ± 0.11 Fe/dimer) recorded at 12.0 K (black trace). The 10.5 K EPR spectrum for photoreduced HydF (red trace) following an anaerobic thaw/freeze event (72 μM protein at 2.54 ± 0.04 Fe/dimer).

Table S1. Reported EPR spectroscopic g-values for $[2Fe\text{-}2S]^+$ and $[3Fe\text{-}4S]^+$ cluster signals. Values obtained via simulation with EasySpin as described in the main body.

Enzyme	Cluster	Temperature	g_1	g_1-strain	g_2	g_2-strain	g_3	g_3-strain
Freshly purified HydF	$[2Fe\text{-}2S]^+$	12 K	2.010	0.010	2.002	0.013	1.963	0.024
	$[2Fe\text{-}2S]^+$	30 K	2.010	0.009	2.002	0.012	1.963	0.025
As-isolated HydF	$[2Fe\text{-}2S]^+$-A	30 K	2.010	0.011	2.003	0.012	1.961	0.018
	$[2Fe\text{-}2S]^+$-B	30 K	2.045	0.015	2.008	0.017	1.981	0.024
	$[3Fe\text{-}4S]^+$	15 K	2.019	0.028	2.010	0.022	1.974	0.044
Freshly purified HydF Photoreduced	$[2Fe\text{-}2S]^+$	30 K	2.010	0.009	2.005	0.011	1.960	0.020
HydE	$[2Fe\text{-}2S]^+$	12 K	2.007	0.013	2.004	0.020	1.955	0.037
	$[3Fe\text{-}4S]^+$	12 K	2.027	0.009	2.014	0.010	1.988	0.042
	$[2Fe\text{-}2S]^+$	30 K	2.008	0.025	2.006	0.010	1.959	0.031
PFL-AE	$[3Fe\text{-}4S]^+$	12 K	2.030	0.010	2.009	0.011	1.988	0.031
	$[3Fe\text{-}4S]^+$	30 K	2.035	0.019	2.008	0.017	1.993	0.023
	$[2Fe\text{-}2S]^+$	30 K	2.010	0.011	2.005	0.011	1.964	0.016

A. Primary $[2Fe\text{-}2S]^+$ cluster signal. B. Low intensity paramagnetic cluster signal assigned as arising from a $[2Fe\text{-}2S]^+$ cluster signal given its slow temperature relaxation properties (Figure S4).

Table S2. EPR spin integrations for HydF and PFL-AE iron sulfur cluster signals.

Enzyme	Cluster	Conditions	Temperature (K)	Spin
HydF	$[2Fe\text{-}2S]^+$	Freshly Purified	12	0.03 – 0.05[a]
			25	0.08
		Freshly Purified + Dithiothreitol	16	0.20
			30	0.27
		Freshly Purified + Dithionite	12	N/A
		Reconstituted+ Dithiothreitol	12	0.15 – 0.19[a]
HydF	$[4Fe\text{-}4S]^+$	Freshly Purified[b]	12	0.34 – 0.38[a]
		Freshly Purified + Dithionite	10.5	0.53
PFL-AE	$[2Fe\text{-}2S]^+$	As-isolated	30	0.08

[a] Reported spin integration range is for two independently made enzyme samples. [b] Samples were photoilluminated for 1 hr in the presence of 5-deazariboflavin. N/A, Not applicable.